

Regular article

Grain boundary mediated plasticity: The role of grain boundary atomic structure and thermal activation

D. Terentyev^{a,*}, A. Bakaev^a, A. Serra^b, F. Pavia^c, K.L. Baker^d, N. Anento^b^a SCK-CEN, Nuclear Materials Science Institute, Boeretang 200, B-2400 Mol, Belgium^b Departament of Civil and Environmental Engineering, E.T.S. Enginyeria de Camins, Universitat Politècnica de Catalunya (UPC), BarcelonaTech, Jordi Girona 1-3, 08034 Barcelona, Spain^c ANSYS Switzerland GmbH, Technoparkstrasse 1, CH-8005 Zürich, Switzerland^d Ecole Polytechnique Federale de Lausanne, Lausanne, Switzerland

ARTICLE INFO

Article history:

Received 19 July 2017

Received in revised form 26 September 2017

Accepted 4 October 2017

Available online 7 October 2017

Keywords:

Dislocations

Grain boundary

Plasticity

ABSTRACT

The interaction of dislocation pile-ups with several tilt grain boundaries (GB) is studied in copper by using a hybrid continuum-atomistic approach. The effects of temperature, pile-up intensity and GB structure on absorption and transmission of slip as a function of local stress state are explored. By considering several high-angle GBs with different misorientation angles, we demonstrate that GB atomic structure primarily defines its ability to accommodate incoming pile-up dislocations, thus limiting the direct transmission of pile-ups through the interface.

© 2017 Acta Materialia Inc. Published by Elsevier Ltd. All rights reserved.

Mechanical response of structural materials, naturally being polycrystalline, is defined by a number of key physical processes where grain boundaries (GBs) play an important role as bulk dislocations. The initiation of plastic deformation is controlled by dislocations, their multiplication and interaction with strengthening defects, while sustainability and capacity of controlled deformation is defined by the uniform propagation of slip through grains [1,2]. Recent experiments involving nano-twinned pure copper (Cu) show that the presence of nanometer-thickness nano-twins offers an exceptional combination of strength and ductility [3,4], suggesting that specific GBs may improve not only strength but ductility as well. To rationalize these results, the interaction of dislocation pile-up (DPU) – inevitable upon severe plastic deformation – with several symmetric tilt grain boundaries (STGB) was studied [5–8]. Direct atomistic simulations provided rich details on local structural transitions occurring as the DPU impinges on the GB interface, and helped to extend the Lee–Robertson–Birnbbaum criteria by accounting for local stress-field at the GB due to the pile-up [5]. However, these studies are limited to zero temperature and so far consider only highly ordered STGBs.

In real structural materials such as austenitic or aluminum/copper-based alloys, widely applied in automotive, aerospace and nuclear industries, grain boundaries have variety of structures including both symmetric and general. Degradation of mechanical properties of these materials in service is often observed along with occurrence of slip-band localization – formation of defect free channels (e.g. [2,9–12]),

suggested to be ‘cleaned’ by dislocation glide (e.g. [13,14]). Propagation of slip-bands through grain boundaries makes material macroscopically heterogeneous, leading to premature failure and detrimental loss of ductility [2]. Post deformation experiments, however, indicate that certain GBs transmit slip-bands, while some arrest and deflect them. Hence, the role of GB atomic structure in the GB-slip band interaction needs to be further clarified. Here, we model dislocation pile-up impinging at STGBs with principally different structures and clarify the role that thermal activation and strain rate sensitivity play in the dislocation transmission. FCC copper is considered here because it may serve as a model material for Cu-based alloys and austenitic stainless steels as well as complement fine-scale micro-mechanical experiments for pure Cu.

A hybrid atomistic/discrete-dislocation model was applied to simulate the DPU-GB interaction. Rather than use a concurrent coupling [15], the hybrid approach uses separate continuum and atomistic simulations that define mutual boundary conditions. The method solves for the positions of continuum dislocations in a pile-up as a function of an externally-applied shear stress σ_{app} and with the positions of any dislocations in the atomistic region held fixed at the atomistically-determined positions. The displacement field of the continuum pile-up is then used to define displacement boundary conditions on the (much smaller) atomistic simulation cell. The stress state on the GB due to those dislocations not at the GB was also computed. The atomistic region is then evolved by molecular dynamics at 0 K and finite temperature. New dislocation positions are identified using a lattice statistical analysis developed especially for high temperature simulations [16]. If no transmission or grain boundary dislocation GBD creation occurs,

* Corresponding author.

E-mail address: dterenty@sckcen.be (D. Terentyev).

the atomistic dislocation positions are then exported back into the continuum level simulation to obtain a new pile-up configuration. When any transmission or GBD creation occurs, the simulation is halted and the event characterized in terms of the local stress state at that instant. Schematics of the method, details of the simulation procedure, and demonstration of its application are provided in Supplementary material Part A (general scheme) and Part B (relation between external load and normal/shear stress at the head of a pile-up).

The simulation cell consisted of a symmetric Cu bicrystal with an initially coherent STGB interface in the middle. Approximate dimensions of the cell size were $40 \times 30 \times 10$ nm with a total number of atoms ~ 1 M. Periodic boundary conditions were imposed along the $\langle 121 \rangle$ tilt axis (coincide with z axis in MD setup), with fixed boundaries in the other two directions as dictated by the continuum solution at the applied stress σ_{app} increases. y axis is normal to the GB plane, and x axis is contained in the GB plane being normal to the tilt axis. We studied the $\Sigma 11(113)$ STGB and the three GBs vicinal to it, namely: $\Sigma 321(7,8,-23)$; $\Sigma 237(4,5,-14)$ and $\Sigma 73(3,4,-11)$ that are formed by segments of $\{113\}$ boundary separated by the GBDs necessary to accommodate the increase of the misorientation angle (which is 66.3° , 68.46° and 69.97° , respectively). The Burgers vector of the GBD in the $\Sigma 321(7,8,-23)$; $\Sigma 237(4,5,-14)$ GB's is $b_g = a_0/2/11[113]$ perpendicular to the GB. The analysis of the Burgers vector was realized by construction of the dichromatic pattern (see, for example, the $\Sigma 11(113)$ STGB in Supplementary material Section C). The $(3,4,-11)$ GB represents a limiting case where the segments of $\{113\}$ boundaries are reduced to the minimum length, and the boundary is thus formed by alternate steps corresponding to the cores of these GBDs. In Fig. 1, the relaxed atomic structures of these STGBs are shown, and the cores of the intrinsic GBD's (denoted "nodes" hereafter) are clearly seen. In the following we refer to the core regions as 'disconnections' to the GBD with step character. A similar type of defect was called a "displacement shift coincidence" by Yu et al. [8], however our term is more general.

The pile-up is introduced along the $\{111\}$ glide plane inclined at $\sim 60^\circ$. The bicrystals were relaxed using the conjugate gradient method and then atomic displacements corresponding to an initial σ_{app} (25 or 100 MPa) were applied to all the atoms. The crystal was relaxed again and thermalized for 10 ps to achieve a desired initial temperature. The loading was realized by updating atomic positions of the fixed boundaries to mimic the increase of σ_{app} in increments of 10–25 MPa depending on temperature. The loading rates used were 10^6 and 10^7 s $^{-1}$, typical for large scale MD simulations of dislocations. The fixed integration MD time step was taken as 2.5 fs for all runs, given that the upper simulation temperature was 300 K. For $T = 0$ K, an incremental

relaxation was performed to achieve convergence of force to 0.1 eV/Å/atom. The interatomic interactions were modeled by using the embedded-atom method (EAM) potential for Cu by Mishin et al. [17], developed on the basis of ab initio calculations and experimental data for elastic constants, point defects and stacking-fault energy. Previously, FCC Cu was successfully used as a model for low SFE austenitic steels to study dislocation-mediated plasticity in the presence of radiation defects [18–20].

Dislocation transmission and dislocation absorption (accompanied with and without creation of GBDs, called yielding) were observed depending on the loading conditions and GB type. These mechanisms were registered by means of atom-core visualization, as demonstrated in Fig. 1 (lower panel). For the highly ordered GB e.g. $\Sigma 11(113)$, the absorption was realized via the split of the first incoming dislocation (ICD) into a residual dislocation and a disconnection, see Fig. 1e and the animation in the Supplementary material. The disconnection advances along the interface as σ_{app} increases, as described in detail previously [5].

For the GBs containing nodes, e.g. $(4,5,-14)$ GB, movement of disconnections was inhibited by the nodes, and initiation of GB yield was observed only in finite temperature simulations. In our simulations, the resistance of the nodes against disconnection slip was significantly higher for $(7,8,-23)$ and $(3,4,-11)$ GBs where no GBD movement was observed at either 0 K or finite temperature. It should be noted that, in the case of $(7,8,-23)$ GB, the ICD was in the neighborhood of the node, which is also always the case for the $(3,4,-11)$ GB. Thus, in the $(7,8,-23)$ GB, the stress concentration induced by the dislocation pileup eventually led to transmission, as illustrated in Fig. 1(h, i). The transmission reaction proceeds via the constriction and re-emission of a $1/6 \langle 112 \rangle \{111\}$ partial into the neighbouring grain, see Supplementary animation. In this case the aforementioned decomposition into a residual dislocation and a disconnection does not occur because of the presence of the nearby node. Instead, the conservation of Burgers vector is accomplished by the reaction $1/6 \langle 112 \rangle \{111\} = 1/6 \langle 112 \rangle \{111\} + 1/22 \langle 741 \rangle$, where the latter Burgers vector is a disconnection that creates a GB step (as defined from the dichromatic pattern shown on Fig. C in the Supplementary material).

For both mechanisms, bulk partial, GBD partial, stacking faults, and GB interface plane are clearly distinguished using the visualization method. By following the interaction mechanism, we have identified the loading state and computed the resolved shear and normal stress components for (i) initiation of GB yield, (ii) transmission events, and (iii) complete absorption of the ICD.

The resolved shear stress exerted on the ICD (shear stress in the grain boundary plane) at the moment of absorption is shown in Fig. 2

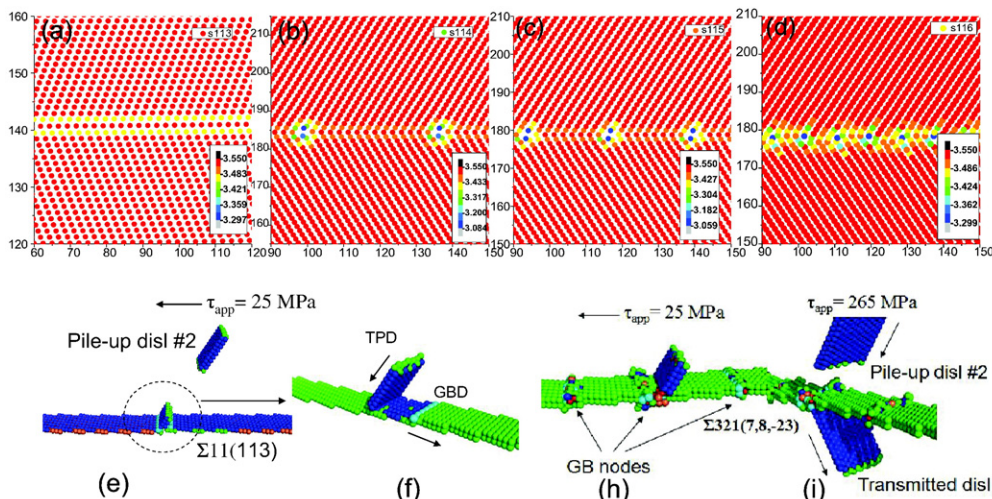


Fig. 1. Upper bar figures present atomic structure and cohesive energy map for the four studied STGBs (a) $\Sigma 11(113)$, (b) $\Sigma 321(7,8,-23)$; (c) $\Sigma 237(4,5,-14)$ and (d) $\Sigma 73(3,4,-11)$. Figs. e-i present the mechanism of dislocation absorption (e & f) and dislocation transmission (h & i) as seen by atom-core visualization analysis.

as a function of temperature. The absorption at the ‘yielding’ GBs occurs for much lower σ_{xy} because no constriction is required to ‘pump in’ the ICD. Moreover, σ_{xy} is reduced significantly with increasing temperature, which points to the low activation barrier for overcoming the resistance to shearing of the GB interface by the moving a GBD. In the GBs where the disconnections are sessile, σ_{xy} is ~ 1 GPa at 0 K and reduces to only ~ 800 MPa at finite temperature and essentially independent of loading rate. Hence, the dislocation absorption (accommodation on the GB interface) at the ‘non-shearable’ GBs is defined by the force balance needed to achieve constriction of the ICD pinned by the GB interface.

The highly disordered GBs can therefore be used to investigate the stress-state conditions for the dislocation transmission, while plastically deformable GBs are good to identify GB yield locus, as was done for aluminum in [5]. We plotted the compressive vs. resolved shear stress for the absorption and transmission events in Fig. 3. This figure basically summarizes the results of the simulations involving different temperature, loading rate and number of dislocations in pile-up. The latter is the crucial parameter because its variation allows one to control σ_{xy}/σ_{yy} ratio (see plots σ_{xy} vs. σ_{app} and σ_{yy} vs. σ_{app} in Supplementary material Section B) and force the system towards transmission or absorption pathway.

The GB yield locus, drawn in Fig. 3, is obtained using the data for $\Sigma 11(113)$, as it never shows transmission at finite temperature. To provide a comparison with previous works, we have added the GB yield locus deduced in [6] for the $\Sigma(113)$ in Al, and find notable agreement. This is not surprising since the structure of the $\Sigma 11(113)$ GB and GB yield mechanism studied in Al [5] are identical to those found here in Cu. The other point where we reached quantitative agreement is the critical amount of dislocations to initiate transmission in $\Sigma 11(113)$ at 0 K, which was found to be >6 in [8] for the same geometry as studied here. At finite temperature, no transmission could be achieved because the stress-concentration was dynamically ‘dissolved’ by moving GBDs.

The transmission locus in Fig. 3 is drawn using data for the (7,8,-23) and (3,4,-11)GBs. This is a principally new result, not reported so far, to our knowledge. It is drawn for the range of σ_{xy} and σ_{yy} between 0.5 and 1 GPa. In this range, the transmission occurs for conditions $\sigma_{yy} > 1.15 \times \sigma_{xy}$ and $\sigma_{yy} \geq 600$ MPa. Apparently, such conditions can be met only if the stress-concentration due to an inclined pile-up keeps increasing and is not relieved by the GB yielding. As demonstrated here, the latter process is strongly suppressed in highly disordered GBs and transmission is inevitable even at the highest studied temperature.

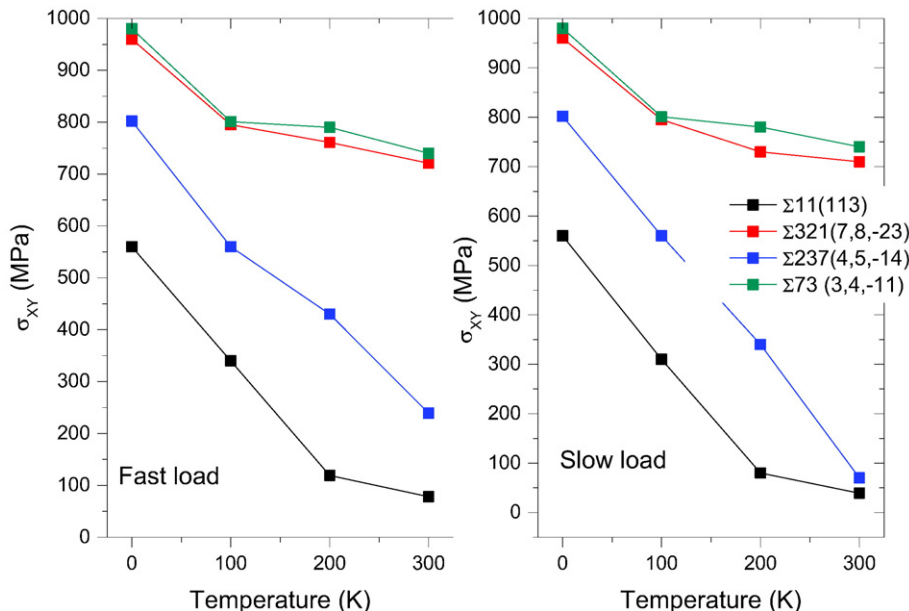


Fig. 2. Shear stress exerted on the first dislocation to initiate its absorption as a function of temperature for the two loading rates.

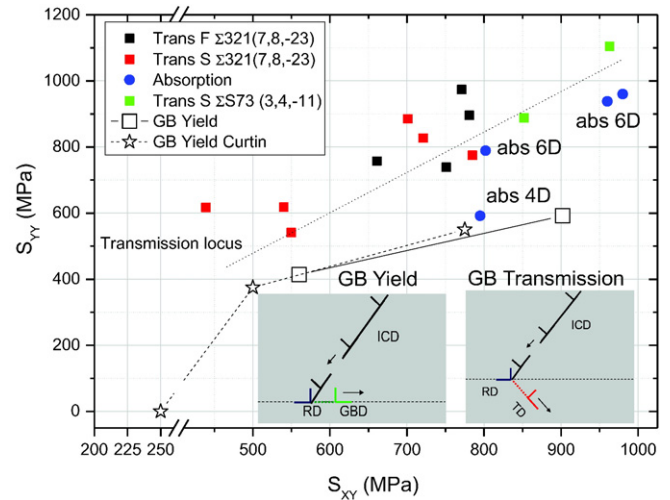


Fig. 3. GB transmission and yield loci relating normal and shear stress exerted on the dislocation pinned at GB interface. Any point above ‘transmission locus’, obtained using data for $\Sigma 321(7,8,-23)$ and $\Sigma 73(3,4,-11)$ GBs, will result in the nucleation of dislocation in the neighbouring GB. GB yield locus is obtained using data for $\Sigma 11(113)$ and $\Sigma 237(4,5,-14)$ GBs. The GB yield locus for $\Sigma 11(113)$ in Al from [4] is added for comparison. Two schematic inset figures demonstrate difference between GB yield and transmission.

We therefore conclude that atomic-scale core structure defines properties of GB dislocations, their glide modes, lattice resistance, and as a global consequence the ability of highly-ordered GBs to arrest slip-bands by dissolving dislocations arriving from pile-ups. Such behaviour naturally explains experimentally observed super plasticity in nano-twinned copper [3,4], as highly ordered twins are known to easily accommodate plastic deformation. High resistance of GBs against interface plasticity, expected in random GBs, should assist/favor dislocation transmission, and hence allow for dislocation and, consequently, slip-band propagation. Note that modification of ‘shearable’ GBs by e.g. segregation or precipitation, typically observed under thermal ageing or irradiation of structural steels, must inevitably lead to the suppression of GB plasticity, hence removing the attractive capability of arresting channels. As a result, even fine-scale chemical re-arrangement at GB cores may have detrimental effects expressed in the premature failure by

inhomogeneous deformation via slip-band nucleation and propagation. The alternation of the deformation behaviour from slip to crack initiation, induced by the incapability of grain boundaries to accommodate or transfer the slip, was very recently confirmed by the microstructural characterization of slip-band evolution in austenitic steels after irradiation [11].

The above described picture on the role of GB plasticity provides a numerical framework to rationalize the well-known GB-related effects (e.g. non-equilibrium precipitation, gas bubble growth or interstitial impurity segregation), all of which lead to the so-called grain boundary embrittlement phenomenon. Unlike previous speculations based on the reduction of the cohesive strength due to the above listed GB-effects, one should address the reduction of GBD-mediated plasticity that drives accumulation of a critical stress concentration sufficient to initiate micro-cleavage. Hence, the investigation of GB dislocations, their structure and dynamic characteristics must be the next step towards understanding of the interaction of GBs with dislocation pile-ups or slip-bands.

To summarize, we have studied the interaction of dislocation pile-ups with several STGBs in FCC Cu using hybrid atomistic-continuum simulation model. As a result, we computed the stress-state corresponding to two types of interaction mechanisms: dislocation transmission and GB yield via dislocation absorption and glide. For the first time, the effect of temperature on GB plasticity and subsequent evolution of stress-concentration was explored for several STGBs with different misorientation angles.

Simulations at 0 K have confirmed that highly ordered $\Sigma 11(113)$ GB exhibit low resistance against GB slip, and therefore the interaction with a pile-up results in the nucleation of a mobile GBD, in agreement with previous works in Al and Cu. The absorption of the leading pile-up dislocation at the other three GBs required remarkably higher shear stress in the pile-up glide plane and no GB plasticity was observed.

Simulations at finite temperature demonstrate that GB slip may also take place on the $\Sigma 237(4,5,-14)$ GB, however, the nodes act as obstacles limiting the glide of GBDs. In the case of $\Sigma 321(7,8,-23)$ and $\Sigma 73(3,4,-11)$ GBs, the resistance of the interface was so strong that transmission was seen to operate in all the studied conditions. Increasing temperature from 100 K up to 300 K and reduction of loading rate by one order of magnitude practically did not change the applied shear stress necessary to initiate dislocation transmission through these GBs. For the other GBs, the resolved shear stress to initiate the GB yield exhibits almost linear drop down to tens of MPa at room temperature.

It is shown that the GB core structure primarily defines its ability to accommodate incoming pile-up dislocations on the GB interface. Dynamic dislocation re-arrangement prevents accumulation of stress-

concentration at the intersection of pile-up and GB interface, so for shearable GBs one cannot accumulate critical stress concentration to initiate dislocation transmission. In the highly disordered GBs, where slip is totally suppressed, the conditions for the dislocation transmission are deduced.

Acknowledgements

Help of Prof. William Curtin is greatly acknowledged! This work has been carried out within the framework of the EUROfusion Consortium and has received funding from the Euratom Research and Training Programme 2014–2018 under grant agreement no. 633053. Support for K. L. Baker was provided through ERC Grant No. 339081. The project M4F GA 755039 and the Spanish project FIS2015-69017-P are acknowledged as well.

Appendix A. Supplementary data

Supplementary data to this article can be found online at <https://doi.org/10.1016/j.scriptamat.2017.10.002>.

References

- [1] A. Sutton, R. Balluffi, *Interfaces in Crystalline Materials*, Clarendon Press, Oxford, 1996.
- [2] G.S. Was, *Fundamentals of Radiation Materials Science*, Springer, New York, 2007.
- [3] L. Lu, Y.F. Shen, X.H. Chen, L.H. Qian, K. Lu, *Science* 304 (5669) (2004) 422–426.
- [4] M. Dao, L. Lu, Y.F. Shen, S. Suresh, *Acta Mater.* 54 (20) (2006) 5421–5432.
- [5] M.P. Dewald, W.A. Curtin, *Model. Simul. Mater. Sci. Eng.* 15 (1) (2007) S193–S215.
- [6] M.P. Dewald, W.A. Curtin, *Philos. Mag.* 87 (30) (2007) 4615–4641.
- [7] M. Dewald, W.A. Curtin, *Model. Simul. Mater. Sci. Eng.* 19 (5) (2011).
- [8] W.S. Yu, Z.Q. Wang, *Acta Mater.* 60 (13–14) (2012) 5010–5021.
- [9] J. Polak, M. Sauzay, *Mater. Sci. Eng., A* 500 (1–2) (2009) 122–129.
- [10] W. Zielinski, W. Swiatnicki, M. Barstch, U. Messerschmidt, *Mater. Chem. Phys.* 81 (2–3) (2003) 476–479.
- [11] B. Cui, J. Kacher, M. McMurtrey, G. Was, I.M. Robertson, *Acta Mater.* 65 (2014) 150–160.
- [12] G.S. Was, D. Farkas, I.M. Robertson, *Curr. Opin. Solid State Mater. Sci.* 16 (3) (2012) 134–142.
- [13] T. Diaz de la Rubia, H. Zbib, T. Khraishi, B. Wirth, M. Victoria, M. Caturla, *Nature* 406 (2000).
- [14] N.M. Ghoniem, S.H. Tong, B.N. Singh, L.Z. Sun, *Philos. Mag. A* 81 (11) (2001) 2743–2764.
- [15] L.E. Shilkrot, R.E. Miller, W.A. Curtin, *Phys. Rev. Lett.* 89 (2) (2002).
- [16] D. Terentyev, P. Grammatikopoulos, D. Bacon, Y. Osetsky, *Acta Mater.* 56 (2008) 5034–5046.
- [17] Y. Mishin, M. Mehl, D. Papaconstantopoulos, *Phys. Rev. B* 63 (2001) 224106.
- [18] T. Nogaret, C. Robertson, D. Rodney, *Philos. Mag.* 87 (6) (2007) 945–966.
- [19] J. Robach, I. Robertson, H. Lee, B. Wirth, *Acta Mater.* 54 (2006) 1679–1690.
- [20] Y.N. Osetsky, D.J. Bacon, *Mater. Sci. Eng.* (2005).